Studies on the Self-Assembly Behavior of the Hydrophobically Associating Polyacrylamide

Hong Chen,[1] Zhongbin Ye,[1,2] Lijuan Han,[1,2] Pingya Luo[1]

[1]*State Key Laboratory of Oil and Gas Reservoir Geology and Exploitation, Southwest Petroleum University, Chengdu 610500, People's Republic of China*
[2]*School of Chemistry and Chemical Engineering, Southwest Petroleum University, Chengdu 610500, People's Republic of China*

Received 18 February 2011; accepted 27 April 2011
DOI 10.1002/app.34756
Published online 24 August 2011 in Wiley Online Library (wileyonlinelibrary.com).

ABSTRACT: Contrasted with partially hydrolyzed polyacrylamide (HPAM), the self-assembly behavior and microstructure of hydrophobically associating polyacrylamide (HAPAM) in aqueous solution have been studied by means of fluorescence spectrum, transmission electron microscopy (TEM), atomic force microscope (AFM), and apparent viscosity test in this article. The fluorescent probe analysis indicates that the HAPAM molecules will form associating aggregates in pure water. The results show that HAPAM can easily self-assemble to form an aggregate by hydrophobic driving force in dilute aqueous solution. The association of hydrophobic groups of the HAPAM causes the formation of supermolecule, so there are associating aggregates formed at very low concentration and then leads to the formation of network at a higher concentration. TEM and AFM measurements show that a distinct network structure has been formed in 1000 mg L^{-1} of HAPAM solution, indicating the strong association of hydrophobic groups. These results are consistent with the viscosity measurement and reveal that the excellent viscosification of HAPAM is due to the association of hydrophobic groups in the aqueous solution. © 2011 Wiley Periodicals, Inc. J Appl Polym Sci 123: 2397–2405, 2012

Key words: hydrophobic association; hydrophobically associating polyacrylamide; fluorescence spectrum; transmission electron microscopy; atomic force microscope; apparent viscosity

INTRODUCTION

Over the past two decades, hydrophobically associating polymers have attracted considerable attention because of their outstanding solution properties and numerous practical applications.[1–5] Many of these associating polymers are amphiphilic: they contain a hydrophilic main chain with hydrophobic side chains in the molecules. These polymers exhibit a strong tendency to self-associate via inter- or intrapolymeric interactions of the hydrophobic side chains. Water-soluble hydrophobically associating polymers are especially interesting because of their possible applications in food thickeners, coatings, paints, enhanced oil recovery, and water treatment, etc. The hydrophobically modified water-soluble polymers usually consist of a water-soluble backbone onto which a few number of hydrophobic groups have been chemically attached and hydrophobic side groups often consist of long alkyl chains. Even a few of hydrophobic groups on water-soluble polymer backbones can have a profound effect on their properties.[6,7] The viscosification of the traditional polymer relies on its high molecular weight, the expansion, and physical entanglement of polymer chains due to the repulsion of carboxylate groups and hydrogen bonds of amido groups. For hydrophobically associating polymers, strong associations between these hydrophobic units lead to the formation of transient networks that greatly enhance solution viscosity and viscoelasticity, which are reversible and different from crosslinked structures formed by covalent bonds, so these copolymers are sometimes called associative thickeners. In this study, fluorescence spectrum, transmission electron microscopy (TEM), atomic force microscope (AFM), and apparent viscosity measurement have been used to study the self-assembly behavior of the hydrophobically associating polyacrylamide (HAPAM).

Correspondence to: L. Han (hlj@swpu.edu.cn).
Contract grant sponsor: CNPC Innovation Foundation; contract grant number: 2008D-5006-02-05.
Contract grant sponsor: Sichuan Youth Science & Technology Foundation; contract grant number: 08ZQ026-001.

MATERIALS AND METHODS

Materials

HAPAM sample is a copolymer of acrylamide, sodium acrylate, and a polymerizable surfactant

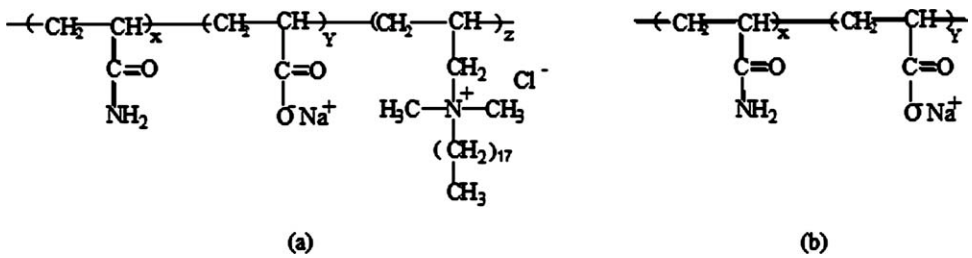

Scheme 1 Chemical structure of HAPAM (a) and HPAM (b).

octadecyl dimethyl allyl ammonium chloride (C_{18}DMAAC) prepared by solution radical polymerization. For comparison, a copolymer hydrolyzed polyacrylamide (HPAM) without hydrophobic comonomer was synthesized under identical conditions. The chemical structure of HAPAM and HPAM are shown in Scheme 1. Water used in this work was distilled.

Concentrated stock polymer solutions were prepared by dissolving appropriate amounts of polymer with distilled water in a 500-mL flask. Gentle magnetic agitation was applied after 1 day of prehydration. The final solution of desired concentration was made up in 50-mL conical flasks by diluting the stock solutions with distilled water and mixing in a thermostatic water bath shaker (25°C) for about 12 h. Before measurements, polymer solutions were left without agitation for at least 1 day to reach equilibrium.

Pyrene was used as fluorescent probe in this study. Pyrene obtained from Aldrich Chemical Co. was recrystallized from absolute ethanol. The stock solutions ($1.0 \times 10^{-4}M$) were prepared in ethanol. A certain amount of stock solution was added to a tube and heated slightly to remove the solvent. Then the final concentration of the probe was adjusted by adding an appropriate amount of the analyte solutions. To dissolve pyrene completely in the hydrophobic microdomains, the solutions were stirred at least overnight before measurement. The pyrene concentration used for the mixture with polymer was $=10^{-6}M$.

Methods

Intrinsic viscosity

The reduced viscosities were measured using a Ubbelodhe capillary viscometer at (30 ± 0.1)°C. The capillary diameter was 0.50 mm. The polymers were dissolved in 1*M* NaCl. The intrinsic viscosities ([η]) were obtained through the Huggins equation as shown below:

$$\frac{\eta_{sp}}{c} = [\eta] + K_H[\eta]^2 c \quad (1)$$

where η_{sp} is the specific viscosity; c is the polymer concentration; K_H is the Huggins coefficient.

Fluorescence measurement

The fluorescence spectra were recorded at room temperature (25°C) using a Cary Eclipse Fluorescence Spectrophotometer. A quartz cell with an optical path of 10 mL was used for the measurements. Both the excitation and emission band slits were kept at 5 nm, and the scan rate was chosen at 300 nm min^{-1}. Three scans were averaged, and the spectra were corrected for Rayleigh and Raman bands in blank polymer solutions. The fluorescence spectra were measured between 350 nm and 550 nm with excitation wavelength at 335 nm.[8] The optimal concentrations and conditions for loading of pyrene into the hydrophobically modified polymers were established.

Transmission electron microscopy

Freeze fracture technique with subsequent TEM is used so as to provide a direct morphology observation of assemblies. TEM micrographs were obtained by using a JEM-100 CX transmission electron microscope (working voltage of 80–100 kV). Replica for TEM observation was prepared by freeze fracture method. To be specific, the sample was frozen in liquid nitrogen before it was fractured in a Balzers BAF-400D etching system at the vacuum less than 10^{-7} bar and etched at a temperature of −120°C. The fracture surface was immediately replicated by first spraying a platinum carbon mixture from an electrode at 45° and then depositing carbon at 90°. Replicas were cleaned in distilled water and then collected on formvar-coated 230 mesh copper electron microscope grids to be observed on TEM.

Atomic force microscope

The samples were deposited on freshly cleaved natural mica, placed in an electrically grounded metal holder and examined directly in the solution, which provides an atomically flat surface, and then dried in air for 24 h to remove the solvent. The samples

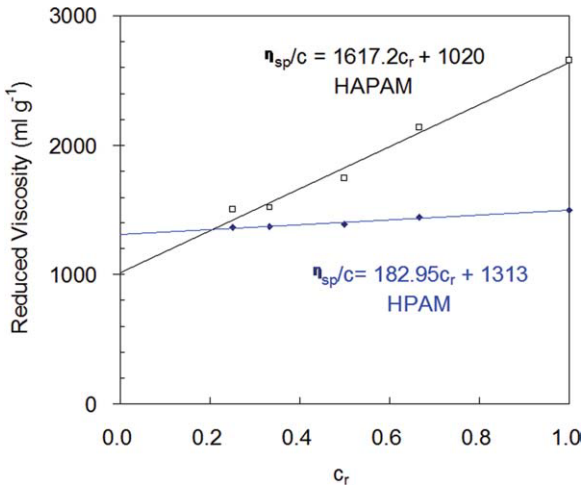

Figure 1 The reduced viscosity as a function of polymer concentration ($c_r = c/c_0$, c is diluted polymer concentration and c_0 is initial polymer concentration). [Color figure can be viewed in the online issue, which is available at wileyonlinelibrary.com.]

were imaged using a Nanoscope IIIa (Digital Instruments, Santa Barbara, CA). It is possible to operate the instrument in two modes; contact and tapping mode. The contact mode drags the sample across the AFM tip and essentially maintains contact between the tip and the sample at all times. The contact method applies a far greater force to the sample and can lead to poor images and distortion of the sample by the tip for soft samples. Alternatively, the tapping mode method operates in a manner where the scanning tip is mechanically oscillated at its resonant frequency. In the tapping mode method, the tip intermittently contacts the surface at the lowest point in the oscillation and this is not in constant contact with the sample. This technique significantly reduces the forces exerted by the tip on the sample compared to the conventional contact mode of operation, thereby reducing sample damage. Integrated silicon cantilevers were used. The cantilevers were oscillated at or slightly below their resonant frequency, which was between 300 and 500 kHz. "Soft" tapping of the surface was achieved by maximizing the tapping mode setpoint, so that it was just below the value required to completely withdraw the tip from the sample. In this way, imaging of the surface layers only was achieved. The samples were scanned using oxide-sharpened Si_3N_4 (8–10 nm) probes.

Apparent viscosity measurement (η_a)

The viscosity properties of samples were measured with a Haake RS 600 rheometer. A double-gap cylinder sensor system is used with an outside gap of 0.30 mm and an inside gap of 0.25 mm. The apparent viscosity of sample is measured at a shear rate 7.34 s^{-1}, and the experimental temperature is 25°C.

RESULTS AND DISCUSSION

Intrinsic viscosity

The intrinsic viscosity [η] and Huggins coefficient were obtained from Huggins equation by Ubbelodhe capillary viscometer method. Assigning the reduced viscosity as the dependent variable and the polymer concentration as the independent variable, a plot of Huggins equation can be made (see Fig. 1). By extrapolating the polymer concentration to zero, the intrinsic viscosity was acquired, and the Huggins coefficient was also acquired by Huggins equation. The results were illustrated in Table I.

From Table I, it can be seen that the intrinsic viscosities of HAPAM and HPAM only have a little discrepancy. However, there exists a great difference in the Huggins coefficients. The Huggins coefficient of HAPAM is much greater than that of HPAM. From Scheme 1 and Table I, we can see that the structure of the HAPAM is nearly the same as the structure of HPAM except that the HAPAM contains a small amount of hydrophobic groups. The hydrophobic groups can self-assemble in aqueous solution, which will enhance the interaction between polymer chain segments. Without the hydrophobic groups of HPAM, the interaction between HPAM molecules is far smaller than that of HAPAM. From Scheme 1and Table I, we can see that the HAPAM contains both anionic and cationic segments. However, it can be likely regarded as an anionic polymer because the amount of the cationic groups is far lower than that of the anionic groups in the polymer of HAPAM.

TABLE I
Physical Parameters of HAPAM and HPAM

Sample	AM (mol %)	NaAA (mol %)	C_{18}DMAAC (mol %)	[η] (mL g^{-1})	H_K	M_η[a] ($\times 10^{-4}$ g mol^{-1})
HAPAM	79.8	20	0.2	1020	5.26	462
HPAM	80	20	0	1313	0.36	634

[a] Calculated from $[\eta] = 4.75 \times 10^{-3} M_\eta^{0.80}$ (Ref. [9]).

Fluorescence measurement

The solubilization of an aromatic hydrocarbon such as pyrene into hydrophobic domain allows one to characterize the structure of amphiphilic polymer in water. Among the various fluorescent probes[10,11] used for characterizing the hydrophobic microdomains, pyrene is most popular and effective because it exhibits a medium-sensitive change in the vibrational fine structure of its emission spectrum. Pyrene is a strongly hydrophobic polyaromatic hydrocarbon with low solubility in water. The high sensitivity of this method facilitates determination of very low critical micelle concentration (cmc) value of micelles. Therefore, pyrene was chosen as probe in this study. Fluorescence emission from amphiphilic compound solution is able to provide more structural and conformational information. Amphiphilic polymers spontaneously form micelles and other ordered structures. The most significant feature of the polymeric micelles is their capability of solubilizing compounds that are otherwise only marginally soluble in water. The small hydrophobic domains present in such solutions are capable of solubilization of pyrene. In systems containing both hydrophobic and hydrophilic phases, pyrene is preferentially solubilized into the former. Excimer fluorescence from pyrene groups terminally attached to the HAPAM allows study of the interactions of polymer.

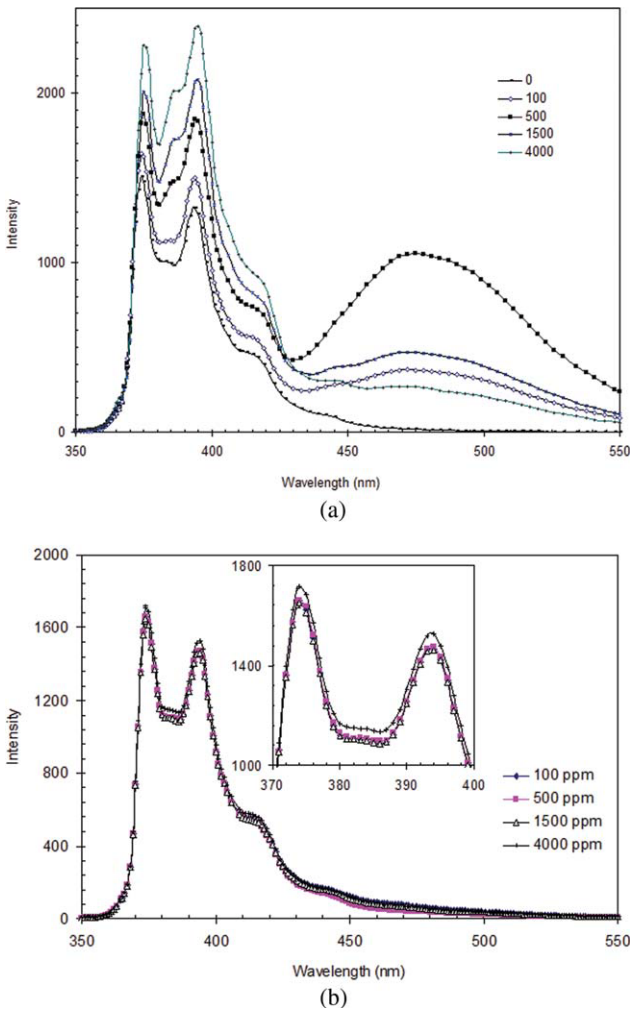

Figure 2 (a) Fluorescence emission spectra of pyrene solubilized in polymer solutions (HAPAM); concentration of polymer, in mg L^{-1}, from top to bottom: 0, 100, 500, 1500, and 4000. (b) Fluorescence emission spectra of pyrene solubilized in polymer solutions (HPAM); concentration of polymer, in mg L^{-1}, from top to bottom: 100, 500, 1500, and 4000. [Color figure can be viewed in the online issue, which is available at wileyonlinelibrary.com.]

Fluorescence spectra

Steady-state fluorescence spectra for pyrene solubilized in various associative polymer concentrations are shown in Figure 2.

It is well known that each fluorescence spectrum of pyrene monomer has 1–5 vibronic peaks from shorter to longer wavelength. There are two regions in the spectra: in the 360–430 nm intervals, vibrational fine structure is present, and at longer wavelengths, there is a broad structureless band with a maximum about at 475 nm. Its fluorescence spectrum presents a fine structure, where the relative peak intensities are highly influenced by the polarity of the solvent molecules by which this probe is surrounded.

In water, the emission is characterized by a broad excimer emission (intensity I_e) centered about at 475 nm and a well-resolved pyrene monomer emission (intensity I_m) at 373 nm. One observes a gradual increase in the intensity of the monomer emission with the increasing of the concentration of HAPAM in Figure 2(a). In addition to the "monomer" emission spectra, one also observes a broad peak at higher wavelength corresponding to the excimer formation due to pyrene molecules in close vicinity in Figure 2(a). This result implies that some hydrophobic microdomains contain more than one pyrene molecule. In Figure 2(b), however, the intensity of the monomer emission with the increasing of HPAM concentration has little change, and a peak of excimer emission spectra is not observed, which means that all pyrene molecules are singly distributed. As the pyrene concentration is similar in both cases, the phenomenon could be attributed to the formation of hydrophobic microdomains in the HAPAM solution.

I_e/I_m

Excimer formation is a well known phenomenon resulting in the self-quenching of excited monomer fluorescence I_m and the rise of a new excited dimer (excimer) emission I_e. The emission of locally

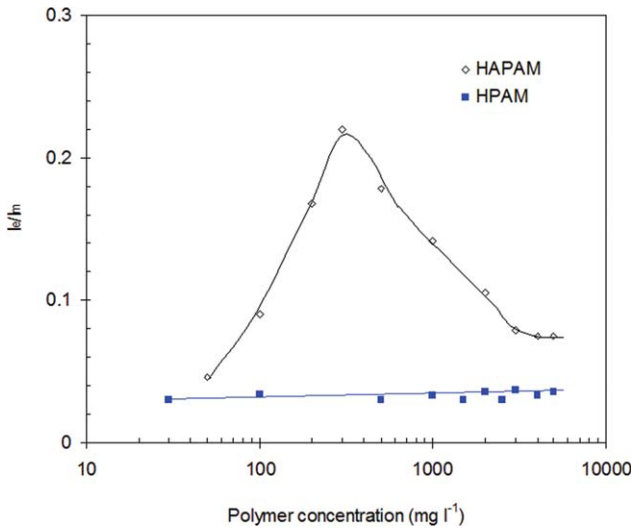

Figure 3 I_e/I_m vs. concentration of polymers. [Color figure can be viewed in the online issue, which is available at wileyonlinelibrary.com.]

isolated excited pyrenes (monomer emission, intensity I_m) is characterized by a well-resolved spectrum at 373 nm. The emission of pyrene excimers[12] (intensity I_e) centered at 475 nm is broad and featureless. Excimer formation requires that an excited pyrene (Py*) and a pyrene in its ground state come into close proximity within the Py* lifetime. Hydrophobic pyrene molecules are exclusively solubilized in the vicinity of hydrophobic chain in these amphiphilic polymers. When there is more than one probe molecule occupying the same micelle, excimer can be formed. The ratio of I_e/I_m is a characteristic of the system that can serve as an indicator of a local concentration of a probe in the micelles.[13] The plots of the ratio I_e/I_m as a function of the concentration of polymer for HAPAM and HPAM are shown in Figure 3.

From Figure 3, it can be seen that the ratio I_e/I_m increases with the increasing of the polymer concentration when the concentration is lower than 300 mg L^{-1} for HAPAM. The reason is that the interaction of hydrophobic group of HAPAM polymer will result in the formation of hydrophobic microdomains or micelles, in which the pyrene can be dissolved and the probability of two pyrene molecules encounter increases with the increasing of the polymer concentration. However, when the concentration is higher than 300 mg L^{-1}, the ratio I_e/I_m decreases with the increasing of the concentration of HAPAM. The hydrophobic microdomain (or micelle) numbers will increase with the increasing of HAPAM concentration. However, the pyrene concentration is constant in the solution. Therefore, when the polymer concentration is high enough, there is only one probe molecule occupying the micelle and the probability of two pyrene molecules encounter decreases resulting in the decrease of the excimer emission intensity in the polymer solution. The local concentration of a probe in hydrophobic microdomain (or micelle) will undergo a maximum with the increase of the HAPAM concentration.

For HPAM, the results are completely different. The ratio of I_e/I_m is almost constant with the increase of the HPAM concentration. The reason is that no hydrophobic microdomain or micelles would form in the HPAM solution and the distribution of the pyrenes in the solution would not be affected by the addition of HPAM.

I_1/I_3

The ratio of the intensities of the first (373 nm) to the third (384 nm) vibronic peak (I_1/I_3) in the emission spectra of the monomer pyrene was used to estimate the polarity of the pyrene microenvironment, the lower the I_1/I_3 ratio, the higher hydrophobic the microenvironment for pyrene. The variation of I_1/I_3 with polymer concentration, therefore, allows one to determine the microenvironment hydrophobicity of the systems.[14] The I_1/I_3 ratio of the intensities of the first and third vibronic peaks in the fluorescence spectrum of pyrene was measured in solutions of HAPAM and HPAM, and the results were shown in Figure 4. The I_1/I_3 ratios report changes in the environment of the pyrene probe.

For HAPAM, at low concentration (50 mg L^{-1}), the I_1/I_3 ratio is about 1.32, which is lower than that of pure water. It indicates that there exist a few hydrophobic aggregates in this concentration range, even if the concentration of polymer was very low. When the concentration is higher than 100 mg L^{-1}, the I_1/I_3 ratios start to decrease significantly. With the increase of HAPAM concentration, more and more hydrophobic microdomains (or micelles) are

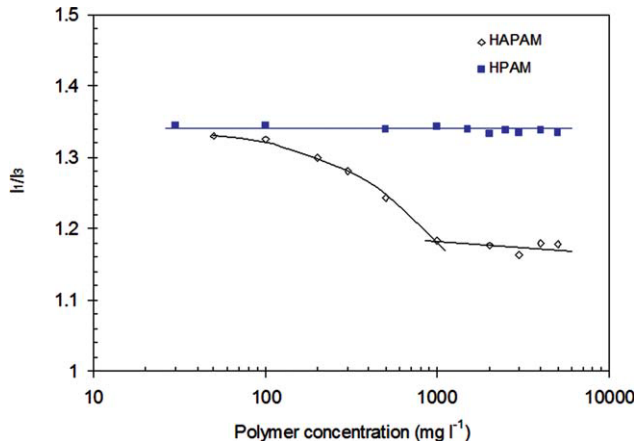

Figure 4 I_1/I_3 vs. concentration of polymers. [Color figure can be viewed in the online issue, which is available at wileyonlinelibrary.com.]

formed by hydrophobic interaction, so that a large number of pyrenes are dissolved into the hydrophobic microdomain (or micelles). When the concentration of HAPAM reaches 1000 mg L^{-1}, it can be seen that there is a turning point. After this turning point, the value of I_1/I_3 has a little change with the increasing of concentration of HAPAM. These phenomena denote that the microstructure of the solution has taken place a great change with the increase of HAPAM concentration. The inflection point (1000 mg L^{-1}) was defined as the critical association concentration (CAC) of HAPAM.

However, it can be seen from Figure 4 that the microenvironment of aggregates in the solution of HPAM is greatly different from that in the solution of HAPAM. With the increase of polymer concentration of HPAM, the value of I_1/I_3 has little change. These results show that almost no hydrophobic microdomains are formed in HPAM aqueous solution. At high concentration of 3000 mg L^{-1}, I_1/I_3 decreases slightly to 1.34, which reflects a slight hydrophobicity of the polymer backbones, leading to the increase in the local concentration of pyrene in domains formed by the aggregation of molecular chains via the interaction of hydrogen bonding.

TEM

Research with TEM requires strict process of specimen preparation, otherwise it is possible to appear severe false image.[15–17] Preparing samples from freeze, etch, and replica under very low temperature was proved a good way to avoid from false image. The microstructures of HAPM and HAPAM were investigated by TEM and the results are shown in Figure 5. Fine and close network structures can clearly be viewed in Figure 5(a) for polymer HAPAM and several layers of overlapped network structures spread throughout the whole solution. The hydrophobic groups attached to the polymer backbone of the HAPAM have very low solubility in water. The micelle-like aggregates formed by hydrophobic association brought about a marked network in the HAPAM solution. Nevertheless, at the same concentration, network structure could not be found in Figure 5(b) for HPAM polymer, only a few polymer clusters is found in the micrograph, which is likely formed by polymer chain entanglement.

AFM

AFM was applied to observe the micromorphology of hydrophobically associating water-soluble polymers solutions.[18–21] The surface of the freshly cleaved mica provided the best combination of imaging features, for example, weakly localized attractive electrostatic forces on a very clean atomically flat surface. A comparative study of the microstructure morphology of HAPAM and HPAM in aqueous solution has been performed with AFM and the results are shown in Figure 6.

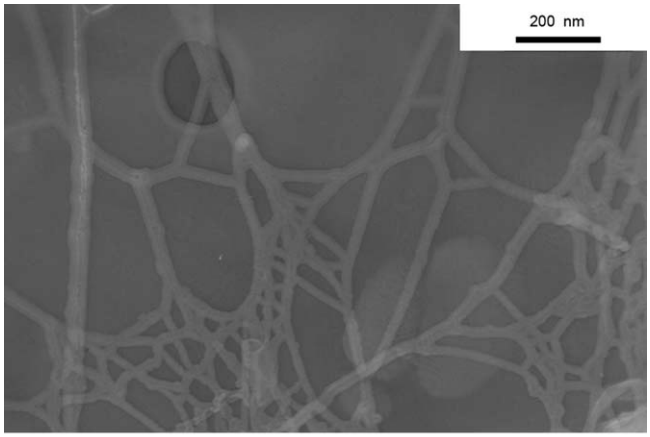

(a)

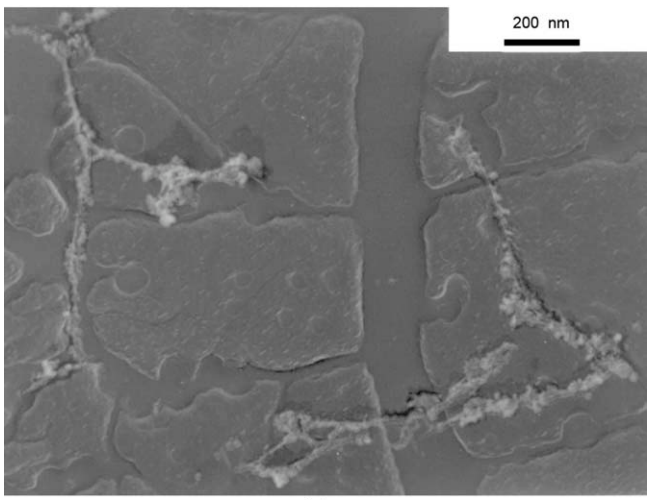

(b)

Figure 5 TEM micrographs of HAPAM and HPAM; (a) HAPAM 1000 mg L^{-1}, (b) HPAM 1000 mg L^{-1}.

When the polymer concentration was 100 mg L^{-1}, there were only sphere aggregates in the AFM micrographs [Fig. 6(a,b)]. When the concentration of the HAPAM increased to 500 mg L^{-1}, many unsymmetrical aggregates were found in Figure 6(c), which were probably formed by the hydrophobic interaction of the HAPAM molecules. However, there were still only sphere aggregates for HPAM in Figure 6(d) at the same concentration except that the mean diameter of the aggregates formed at high concentration was larger than that formed at low concentration [see Fig. 6(b,d)]. When the polymer concentration increased to 1000 mg L^{-1}, an AFM image of the polymer network of HAPAM with concentrated solution above the CAC formed under quiescent conditions was presented in Figure 6(e). The molecular strands of the HAPAM molecules were clearly visible in

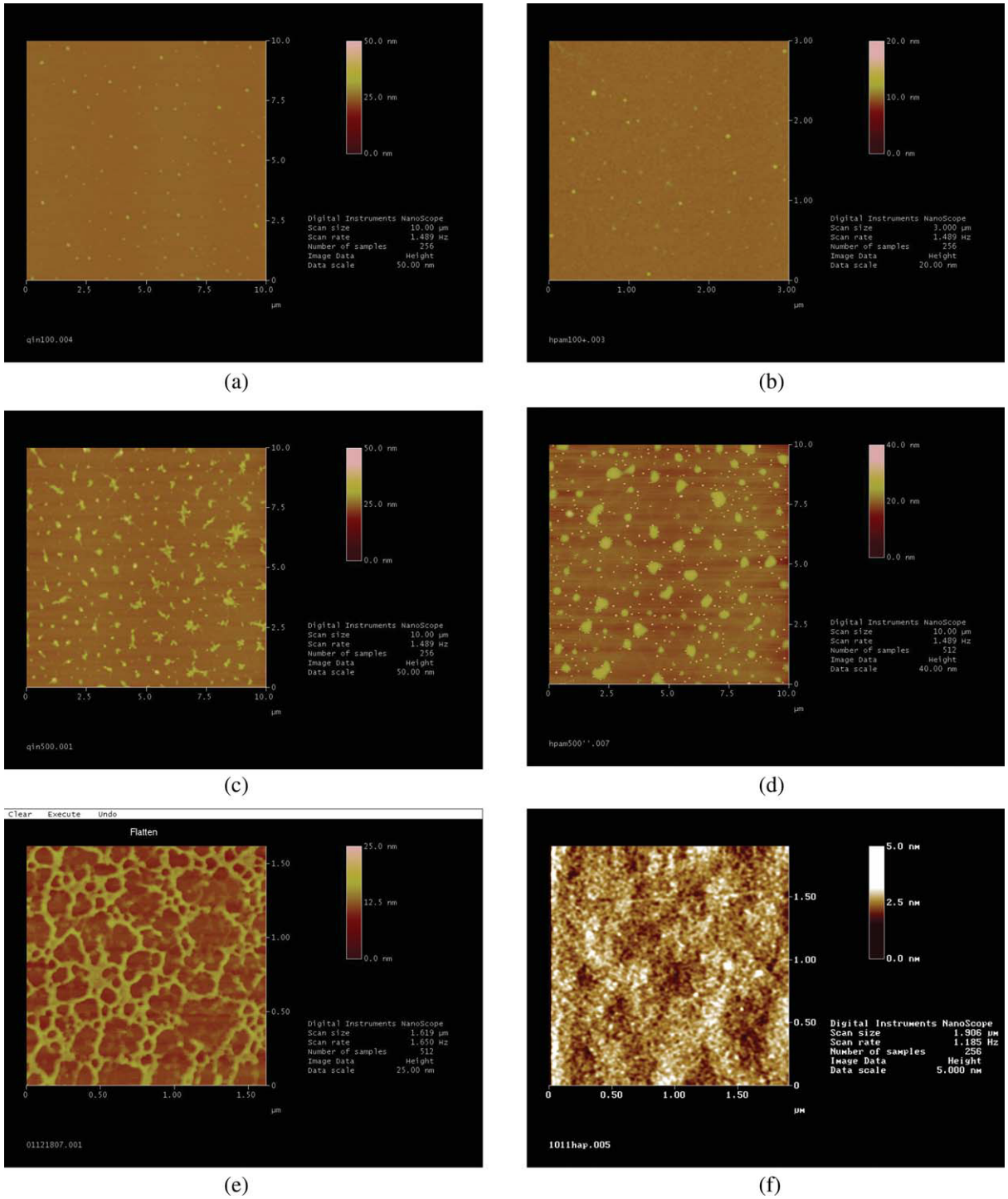

Figure 6 AFM micrographs of HAPAM and HPAM in aqueous solution: (a) HAPAM 100 mg L^{-1}, (b) HPAM 100 mg L^{-1}, (c) HAPAM 500 mg L^{-1}, (d) HPAM 500 mg L^{-1}, (e) HAPAM 1000 mg L^{-1}, (f) HPAM 1000 mg L^{-1}. [Color figure can be viewed in the online issue, which is available at wileyonlinelibrary.com.]

Figure 6(e). While at the same concentration, the molecules of the HPAM would not form three-dimensional network structure in Figure 6(f). HAPAM exhibited a distinct network structure. There was no indication that the substrate surface significantly perturbed or distorted the molecular topology. Images were found to exhibit topological shapes and the results are consistent with the results of TEM studies. Visual observations from AFM in Figure 6(e) confirmed the formation of the three-dimensional network structures of HAPAM in aqueous solution. The network structures spanned in the whole solution were formed resulting in the dramatic increasing of the solution viscosity (see in Fig. 7). The three-

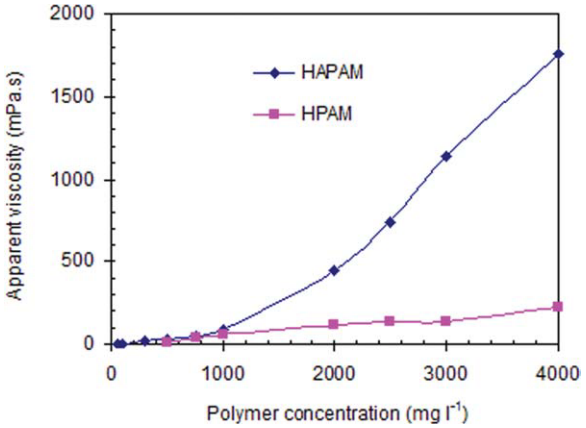

Figure 7 Apparent viscosity vs. concentration of polymers (7.34 s^{-1}). [Color figure can be viewed in the online issue, which is available at wileyonlinelibrary.com.]

dimensional networks distributed in the aqueous solution were formed because of the intermolecular hydrophobic association. The HAPAM molecule chains aggregate together via intermolecular hydrophobic association and the aggregates connect each other to form string-like network bones. Viscosification is likely to occur through entanglement as well as the formation of networks with hydrophobic domains as the junctions. In the polymer solution of HPAM, there were only numerous clusters with different shapes and sizes formed via van der Waals interactions and hydrogen bonding. The results are similar to the observation of TEM.

Apparent viscosity

The viscosities of the HAPAM and HPAM solutions as a function of polymer concentration were plotted in Figure 7.

For HAPAM, a great change appears when the polymer concentration is higher than 1000 mg L^{-1}. Above this polymer concentration, the viscosity of HAPAM increases steeply with the increasing of polymer concentration. The phenomena indicate that the CAC of the polymer is about 1000 mg L^{-1}. The remarkable increase in the apparent viscosity of the HAPAM polymer solution can be attributed to the strong intermolecular associations and the intermolecular bridging. With the increase of HAPAM concentration from 1000 to 4000 mg L^{-1}, the solution viscosity increases from 100 to 1800 mPa s. The results show that the interactions of polymer molecules are reinforced with the increasing of the polymer concentration, resulting in the dramatical increase of viscosity. The fluorescent probe and viscosity measurements show that with the increasing of polymer concentration, above 1000 mg L^{-1} HAPAM, although the nonpolarity of the hydrophobic microdomain tends gradually to be constant, the amount of hydrophobic microdomain and viscosity of the solution increases abruptly because of the remarkable increase of aggregates and the interaction of the aggregates. From the TEM and AFM experiments, we can see that the networks have formed through hydrophobically associating interaction in HAPAM solution when the polymer concentration is above 1000 mg L^{-1}, which can result in sharply increasing of the solution viscosity. The results of viscosity measurement are consistent with those of fluorescent probe, TEM and AFM.

However, almost linear variations were obtained for HPAM solution. The critical concentration of HPAM is not observed in the concentration range investigated. Although the intrinsic viscosity of HPAM is higher than that of HAPAM, the solution viscosity of HPAM is lower than that of HAPAM when at the same concentration.

The difference between the observed results for HAPAM and HPAM in dilute solution can probably be explained by the presence of the hydrophobic groups. In the dilute concentration region, the probability of main chain entanglements for both polymers is quite low. With the increasing of the polymer concentration, hydrophobic groups in different chains will interact with each other and then the associated clusters will serve as stickers to connect each other and to support the framework of the microstructures when the HAPAM concentration is higher than 1000 mg L^{-1}. For conventional water soluble polymers, such as HPAM, the thickening mechanism is depended on the molecular coil expansion increasing the hydrodynamic volume and chain entanglement. For the HAPAM polymer, the thickening through intermolecular entanglement is retained, and another important thickening is derived from a micelle-like association of hydrophobic moieties along the polymer backbone, which can impart unique rheological properties to HAPAM compared to the HPAM.

CONCLUSIONS

The aggregation behavior of HAPAM solution has been investigated by means of fluorescence spectrum, TEM, AFM, and apparent viscosity measurement. The results show that HAPAM exhibits strong association of hydrophobic groups and excellent viscofication properties in aqueous solution. When the polymer concentration is above the critical concentration, the polymers will aggregate each other to form reversible supermolecular structures via intermolecular interaction of hydrophobic groups, resulting in a dramatic increasing of apparent viscosity. So the thickening mechanism of HAPAM is deduced: first, hydrophobic groups associate with

each other and supermolecular aggregates or hydrophobic domains formed; with the increase of polymer concentration, more hydrophobic domains formed; in the end, a space network structure forms in aqueous solution, which results in a dramatic increase in polymer solution viscosity.

References

1. Winnik, F. M.; Regismond, S. T. A.; Goddard, E. D. Langmuir, 1997, 13, 111.
2. Dragan, S.; Ghimici, L. Polymer, 2001, 42, 2886.
3. Ma, J.; Huang, R.; Zhao, L.; Zhang, X. J Appl Polym Sci, 2005, 97, 316.
4. Zhong, C.; Huang, R.; Xu, J. J Solution Chem, 2008, 37, 1227.
5. Zhong, C.; Huang, R.; Ye, L.; Dai, H. J Appl Polym Sci, 2006, 101, 3996.
6. Seigou, K.; Mohd, M.; Kouji, K.; Haruki, M.; Iriany, K.; NorbertH.; Manfred, S. Polym J, 2002, 34, 253.
7. Zhong, C.; Ye, Z.; Luo, P.; Chen, H. Polym Bull, 2009, 62, 79.
8. Alami, E.; Almgren, M.; Brown, W.; Francois, J. Macromolecules, 1996, 29, 2229.
9. National standard GB/T 12005. 10-92, Determination of molecular weight of polyacrylamide by viscometry; Technology Supervision Bureau of PR China, Beijing, 1992.
10. Deo, P.; Deo, N.; Somasundaran, P.; Moscatelli, A.; Jockusch, S.; Turro, N. J.; Ananthapadmanabhan, K. P.; Ottaviani, M. F. Langmuir, 2007, 23, 5906.
11. Horiuchi, K.; Rharbi, Y.; Spiro, J. G.; Yekta, A.; Winnik, M. A.; Jenkins, R. D.; Bassett, D. R. Langmuir, 1999, 15, 1644.
12. Sahoo, D.; Narayanaswami, V.; Kay, C. M.; Ryan, R. O. Biochemistry, 2000, 39, 6594.
13. Vorobyova, O.; Yekta, A.; WinnikM. A.; Lau, W. Macromolecules, 1998, 31, 8998.
14. Bromberg, L. E.; Barr, D. P. Macromolecules, 1999, 32, 3649.
15. Metin, O.; Ozkar, S. Energy Fuels, 2009, 23, 3517.
16. Li, Y.; Zhang, H.; Hu, X.; Zhao, X.; Han, M. J Phys Chem C, 2008, 112, 14973.
17. Shankar, R.; Shahi, V.; Sahoo, U. Chem Mater, 2010, 22, 1367.
18. Eom, K.; Li, P.; Makarov, D. E.; Rodin, G. J. J Phys Chem B, 2003, 107, 8730.
19. Wang, X.; Tu, H.; Braun, P. V.; Bohn, P. W. Langmuir, 2006, 22, 817.
20. Liao, Y.; You, J.; Shi, T.; An, L.; Dutta, P. K. Langmuir, 2007, 23, 11107.
21. Zhong, C.; Luo, P. J Polym Sci Part B: Polym Phys, 2007, 45, 826.